EUROPEAN ORGANIZATION FOR NUCLEAR RESEARCH

CERN–EP–2000–014
31 January 2000

Measurement of the $D_s \to \mu\nu_\mu$ branching fraction and of the D_s decay constant

The BEATRICE Collaboration

Y. Alexandrov[5)], C. Angelini[6)], D. Barberis[3)], F. Ceradini[8)], M. Dameri[3)], G. Darbo[3)], A. Duane[4)], V. Flaminio[6)], B.R. French[2)], C. Gemme[3)], K. Harrison[6)], R. Hurst[3)], C. Lazzeroni[6)], L. Malferrari[1)], G. Martellotti[7)], P. Mazzanti[1)], P. Netchaeva[5)], D. Orestano[8)], B. Osculati[3)], G. Penso[7)], L. Rossi[3)], H. Rotscheidt[2)], D.M. Websdale[4)] and M. Zavertyaev[5)].

Abstract

Using interactions of $350\,\mathrm{GeV}/c$ π^- in copper and tungsten targets, the branching fraction for the leptonic decay $B(D_s \to \mu\nu_\mu)$ is measured to be $(0.83 \pm 0.23_{stat.} \pm 0.06_{syst.} \pm 0.18_{B(D_s \to \varphi\pi)})\%$. The resulting value for the D_s decay constant is $f_{D_s} = 323 \pm 44 \pm 12 \pm 34$.

Submitted to Physics Letters B

[1)] Università di Bologna and INFN, Bologna, Italy.
[2)] CERN, Geneva, Switzerland.
[3)] Università di Genova and INFN, Genoa, Italy.
[4)] Blackett Laboratory, Imperial College, London, United Kingdom.
[5)] Lebedev Physical Institute, Moscow, Russian Federation.
[6)] Università di Pisa and INFN, Pisa, Italy.
[7)] Università di Roma "La Sapienza" and INFN, Rome, Italy.
[8)] Università di Roma "Roma Tre" and INFN, Rome, Italy.

In the quark model, the annihilation rate for the D_s meson's constituent quark and anti-quark is measured by the branching fraction of its (totally leptonic) decay to a lepton and the associated (anti-)neutrino. This decay rate is related to the quark-antiquark wave-function at the origin, which is usually parametrised in terms of the D_s decay constant f_{D_s}.

In the Standard Model, the D_s leptonic branching fraction is given by [1]:

$$B(D_s \to \ell\nu_\ell) = \frac{{G_F}^2}{8\pi}|V_{cs}|^2 f_{D_s}^2 \tau_{D_s} M_{D_s} m_\ell^2 \left(1 - \frac{m_\ell^2}{M_{D_s}^2}\right)^2, \quad (1)$$

where G_F is the Fermi constant, V_{cs} is the CKM matrix element, τ_{D_s} is the D_s lifetime, M_{D_s} and m_ℓ are the masses of the D_s and lepton respectively.

This letter presents the measurement of experiment WA92, where a narrow-pitched silicon microstrip detector, positioned just downstream of the production target, was used to reconstruct the decays of mesons containing heavy quarks and a muon detector selected leptonic decays.

Data taking was performed at the CERN Ω' spectrometer in 1992 and 1993, with a 350 GeV/c π^- beam incident on a 2 mm target of copper or tungsten. The experiment recorded ∼110 million events on Cu (∼50 million in 1992 and the rest in 1993, these hereafter being referred to as the data samples "Cu92" and "Cu93") and ∼40 million events on W (all in 1992, hereafter referred to as the data sample "W92"), corresponding to integrated luminosities of 8.1(nb per Cu nucleus)$^{-1}$ and 1.5(nb per W nucleus)$^{-1}$.

Full details of the experimental apparatus and trigger are given elsewhere [2]. The present analysis relies, in particular, on the imaging capabilities of the high-resolution tracking system. This was made of silicon microstrip planes, arranged as a decay detector (DkD) and a vertex detector (VxD). The DkD, covering the first 3.2 cm downstream of the target, consisted of 17 silicon planes with 10 μm pitch and analogue readout. The VxD consisted of 12 silicon planes of 25 μm pitch, and 5 planes of 50 μm pitch. A beam hodoscope, upstream of the target and comprising ten silicon planes of 20 μm pitch, was used to track the beam particle and helped reconstruct the primary interaction vertex. Tracking further from the target was performed using 58 planes of multiwire proportional chambers in a 1.8 T magnetic field, and 8 planes of drift chambers. A muon detector, consisting of two Fe walls (3.2 m total thickness) and 6 planes of resistive-plate chambers, was positioned downstream of the tracking detectors. It was used to provide a muon trigger signal and allowed reconstructed particles crossing the Fe walls to be flagged as muons.

A combination of several independent triggers [2] was used in order to have a high efficiency for heavy-quark events, with an acceptable dead time. A first-level interaction trigger required the passage of at least two particles in scintillation counters placed downstream of the target, and covering the angular range between 0.75 and 100 mrad, and an energy deposition corresponding to at least 5 minimum-ionising particles in a silicon detector just downstream of the target. An event was written to tape if an interaction trigger was satisfied in coincidence with any two of the following:

i. a high p_{T} trigger, obtained using a pair of butterfly-shaped hodoscopes, crossed only by particles with transverse momentum greater than 0.6 GeV/c;
ii. a muon trigger, requiring the detection in the resistive-plate chambers of a muon consistent with having originated in the target;

iii. an impact-parameter trigger, which used information from the beam hodoscope and the VxD and required reconstruction of at least three primary tracks and two secondary tracks (*i.e.* with impact parameter in the non-bending projection larger than 100 μm).

The number of high-$p_{\rm T}$ particles required at the trigger level was $\geq$1 for the Cu target and $\geq$2 for the W target. In 1993, the muon–high-$p_{\rm T}$ combination was replaced by a muon trigger in coincidence with an impact-parameter trigger requiring three primary tracks and only one secondary track.

For the acceptance calculations, and for studies of backgrounds in the $D_s \to \mu\nu_\mu$ channel, we fully simulated events containing $D_s \to \mu\nu_\mu$, $D \to \mu\nu_\mu$, or production of $c\overline{c}$, and minimum-bias events. The minimum-bias events were generated using Fluka [3]. Events with heavy quarks were generated using Pythia 5.4 [4] and Jetset 7.3 [5] to describe the hard process and quark fragmentation, and using Fluka to determine the characteristics of all other interaction products. Tracking of particles through the experimental apparatus was performed using Geant 3.21 [6].

The trigger acceptance was $\sim 2\%$ for inelastic interactions, $\sim 9\%$ for $c\overline{c}$ and $\sim 22\%$ for events containing $D_s \to \mu\nu_\mu$ and $D \to \mu\nu_\mu$. Details of the trigger acceptance for the different types of simulated events are given in table 1.

Most of the events on tape contained muons from decays in flight of pions or kaons and/or secondary interactions in the silicon detectors. In order to reject most of these events, and to select events containing at least a muon from a heavy quark decay, a fast off-line filter was developed. This took into consideration tracks reconstructed only in the non-bending projection using the VxD, and track segments reconstructed in the muon detector. Vertices were formed from combinations of at least 3 tracks and an event was accepted if it contained at least one vertex in the target and at least one VxD track matching a muon track segment and with the following properties:

i. $p_{\rm T} > 100$ MeV/c in the non-bending projection;
ii. impact parameter larger than 30 μm with respect to any vertices in the target and any vertices with more than 4 tracks;
iii. no energy deposit corresponding to 5 or more minimum-ionising particles less than 30 μm from the extrapolation of the muon-VxD track through the DkD.

The first condition mainly suppressed pion and kaon decays, and the other conditions removed events with secondary interactions, or with multiple primary interactions within the sensitive time of the detectors. The number of events selected by the filter for the W92, Cu92 and Cu93 data sets were respectively 2.5, 2.2 and 2.1 million.

Events passed by the off-line filter were fully reconstructed using a modified version of the reconstruction program Trident [2, 7]. After reconstructing tracks and vertices in three dimensions with the standard WA92 algorithm, kinks were searched for on all tracks not assigned to any vertex. A kink was accepted for further analysis only if the incoming track originated at the primary vertex, which had to be in the target, and the outgoing track had no other track intersect, either in projection or in space, in the neighbourhood of the kink. The energy deposition in the DkD along the incoming and outgoing track was required to be compatible with a single minimum-ionising particle. A further selection procedure was then applied, keeping events containing at least one muon with:

i. $p_{\rm T} > 500$ MeV/c;
ii. impact parameter in the non-bending projection $> 10\,\mu$m, corresponding to 3σ;
iii. impact parameter in space $> 20\,\mu$m and < 1 mm;

Table 1: *Trigger and selection acceptances for events with D_s and D muonic decays, for $c\overline{c}$ events and for minimum bias interactions.*

		$D_s \to \mu\nu_\mu$	$D \to \mu\nu_\mu$	$c\overline{c}$	minimum bias
Interaction trigger	W92	83%	83%	85%	71%
	Cu92	78%	79%	81%	62%
	Cu93	78%	78%	81%	62%
Final trigger	W92	20%	21%	5.8%	1.8%
	Cu92	33%	32%	9.8%	2.2%
	Cu93	18%	20%	7.4%	2.0%
Off-line filter	W92	8.4%	12.6%	1.8%	0.12%
	Cu92	12.1%	15.9%	1.9%	0.10%
	Cu93	8.0%	14.8%	1.6%	0.07%
Selection	W92	0.11%	0.18%	3.0×10^{-5}	6.8×10^{-8}
	Cu92	0.29%	0.38%	4.0×10^{-5}	9.0×10^{-8}
	Cu93	0.31%	0.33%	4.1×10^{-5}	6.9×10^{-8}

iv. a kink between the third and the eleventh plane of the DkD (between 3.8 and 13.4 mm from the downstream edge of the target), *i.e.* at least three hits on each side of the kink;
v. no other track passing near the kink, the minimum track separation being 10 μm in the non-bending projection and 20 μm in the bending projection;
vi. no energy deposition corresponding to the passage of more than five minimum-ionising particles along the muon trajectory or in the neighbourhood of the kink;
vii. p_{T} of the muon relative to the line of flight of the decaying particle larger than 100 MeV/c in each projection.

This selection kept respectively 144, 199 and 205 events of the W92, Cu92 and Cu93 data sets. Most of these events contained semileptonic decays of charged mesons or secondary interactions in the DkD, with low local energy release, followed by a decay in flight of one of the outgoing particles.

Acceptances of the three data samples after application of the off-line filter and the subsequent selection are summarised in table 1. It can be noted that the tighter trigger conditions of the 1993 run resulted in an early rejection of events that would anyway not have passed the off-line filtering and selection. The tighter trigger conditions helped to reduce the dead time of the experiment and thus contributed to the higher final statistics of the Cu93 data set relative to the Cu92 data sample.

The final selection step consisted of a visual inspection of all surviving events. Use was made of an interactive display and analysis program, which allowed rejection of the last few events with a secondary interaction in the DkD. Figure 1 shows an example of such an event. Events were rejected if a local energy release could be seen in the DkD plane closest to the reconstructed kink position and there was an indication of the presence of non-reconstructed low-momentum particles emerging from the "kink" vertex.

After the interactive scanning step respectively 82, 133 and 167 events of the W92, Cu92 and Cu93 data sets survived. The same procedure was applied to the simulated data sets, keeping 81%, 90% and 86% of $D_s \to \mu\nu_\mu$ events, 91%, 93% and 85% of $D \to \mu\nu_\mu$ events and 77%, 89% and 89% of $c\overline{c}$ events. Figure 2 shows one of the $D_s \to \mu\nu_\mu$ candidates.

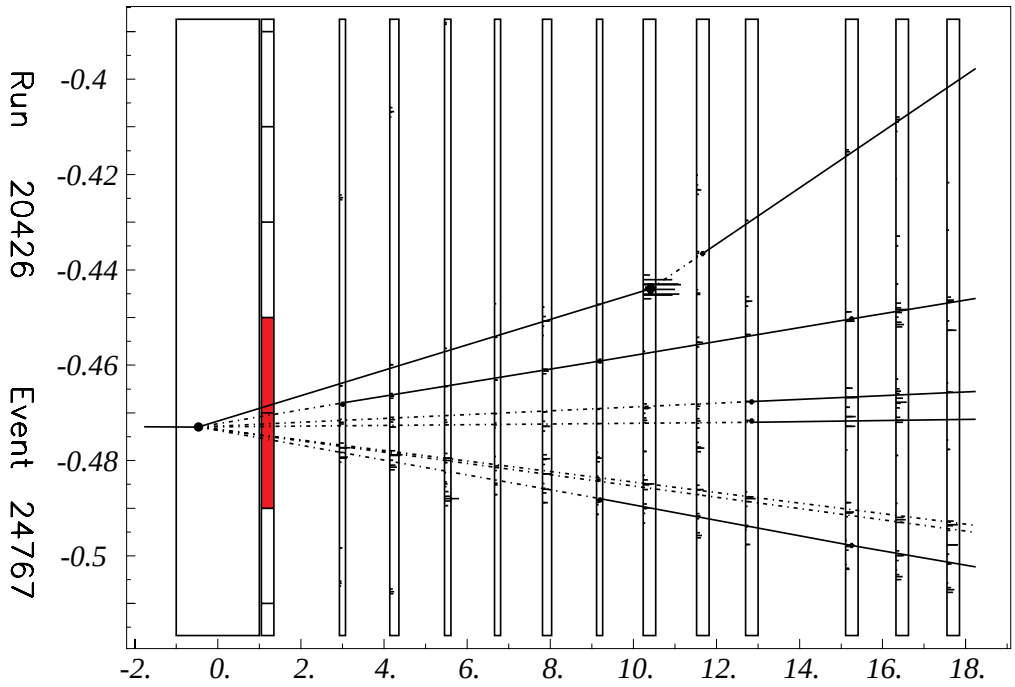

Figure 1: *Display of an event containing a secondary interaction. A particle produced at the primary vertex interacts with the material of one of the DkD planes, releasing some energy near the interaction point. Individual hits are displayed as segments having a length proportional to the pulse height. A non-reconstructed track emerging from the interaction point can also be identified. Scale units are mm; detector planes are shown to scale.*

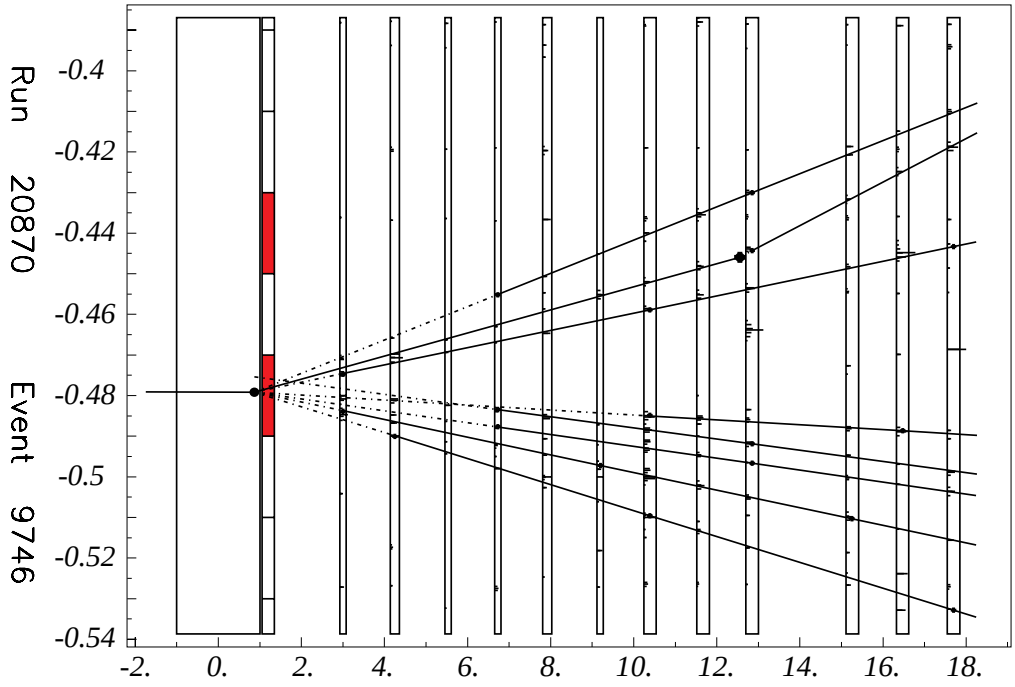

Figure 2: *Display of a $D_s \to \mu\nu_\mu$ candidate. A particle produced at the primary vertex decays to a muon just before the ninth DkD plane, giving a kink. Individual hits are displayed as segments having a length proportional to the pulse height. Scale units are mm; detector planes are shown to scale.*

Discrimination between $D_s \to \mu\nu_\mu$ decays, $D \to \mu\nu_\mu$ decays and charm semileptonic decays can be achieved through a consideration of the variables $p_{\rm TF}$ (transverse momentum of the muon relative to the line of flight of the decaying particle) and $\Delta x/p_\mu$ (distance between the production and decay vertices of the $D_{(s)}$ meson divided by the muon's total momentum). This latter variable is proportional to the proper lifetime for a $D_{(s)} \to \mu\nu_\mu$ decay orthogonal to the line of flight.

Figure 3 shows the distribution of $\Delta x/p_\mu$ versus $p_{\rm TF}$ for the experimental data, for simulated $c\overline{c}$ events, and for the decays $D_s \to \mu\nu_\mu$ and $D \to \mu\nu_\mu$. As these distributions show the same shape for W92, Cu92 and Cu93, data for the three samples were summed in order to increase the statistics. Up to this point the relative normalisation is arbitrary, as many more events were generated by the simulation than were found in the data.

In order to count the number of $D_s \to \mu\nu_\mu$ decays in the experimental data, a binned maximum-likelihood fit using the program Minuit [8] was performed to the $\Delta x/p_\mu$ versus $p_{\rm TF}$ distribution, leaving free only the relative normalisation of the three contributions from $c\overline{c}$ events, $D_s \to \mu\nu_\mu$ and $D \to \mu\nu_\mu$. The decay $D_s \to \tau\nu_\tau$, sometimes followed by $\tau \to \mu\nu_\mu\nu_\tau$, was included in the $c\overline{c}$ sample. Because of the low statistics of the experimental sample, the unconstrained fit procedure did not give a stable result for the relative fractions of $D \to \mu\nu_\mu$ and $D_s \to \mu\nu_\mu$. These fractions can be estimated using the relation:

$$\frac{N^{obs}_{D\to\mu\nu_\mu}}{N^{obs}_{D_s\to\mu\nu_\mu}} = \frac{\sigma(D)}{\sigma(D_s)} \times \frac{B(D \to \mu\nu_\mu)}{B(D_s \to \mu\nu_\mu)} \times \frac{\varepsilon_{D\to\mu\nu_\mu}}{\varepsilon_{D_s\to\mu\nu_\mu}}, \tag{2}$$

where the ratio of branching fractions is given by:

$$\frac{B(D \to \mu\nu_\mu)}{B(D_s \to \mu\nu_\mu)} = \frac{f_D^2}{f_{D_s}^2} \times \frac{\tau_D}{\tau_{D_s}} \times \frac{M_D}{M_{D_s}} \times \frac{|V_{cd}|^2}{|V_{cs}|^2} \times \frac{(1 - m_\mu^2/M_D^2)^2}{(1 - m_\mu^2/M_{D_s}^2)^2}. \tag{3}$$

The ratio of cross-sections was measured in the present experiment using charged hadronic decays of D and D_s mesons, the result obtained being $\sigma(D)/\sigma(D_s) = 2.54 \pm 0.32 \pm 0.69$ [9], with the systematic error dominated by the error on the $B(D_s \to \varphi\pi)$ branching fraction. The ratios of masses, lifetimes and CKM matrix elements have been taken from the current world averages: $M_D/M_{D_s} = 0.9490 \pm 0.0004$, $\tau_D/\tau_{D_s} = 2.263 \pm 0.088$, $|V_{cd}|^2/|V_{cs}|^2 = 0.0512 \pm 0.0016$ [10].

Lattice gauge theories do not yet provide reliable estimates of the pseudoscalar-meson decay constants, but their ratios can be calculated. The ratio of D and D_s decay constants calculated using lattice gauge theory methods is $f_D^2/f_{D_s}^2 = 0.82 \pm 0.09$ [11]. Using this value and the efficiencies described earlier, we have obtained $N^{obs}_{D\to\mu\nu_\mu}/N^{obs}_{D_s\to\mu\nu_\mu} = 0.43 \pm 0.06$ for the W92 data set, 0.31 ± 0.05 for Cu92, 0.24 ± 0.04 for Cu93, 0.27 ± 0.04 for Cu92 and Cu93 combined and 0.29 ± 0.04 for all data sets combined.

Maximum-likelihood fits with $N^{obs}_{D\to\mu\nu_\mu}/N^{obs}_{D_s\to\mu\nu_\mu}$ constrained gave the results shown in table 2. The fits were performed independently for W92, Cu92 and Cu93, then for Cu92 and Cu93 combined, and finally for the three samples taken together. Table 2 shows that the results for the two copper runs are statistically compatible with one another and also with the lower-statistics tungsten run, therefore the value given by the combined fit can be taken as the final result. Figure 4 shows the $p_{\rm TF}$ distribution for all data sets together, with the relative normalisation of the three contributions given by the maximum-likelihood fit.

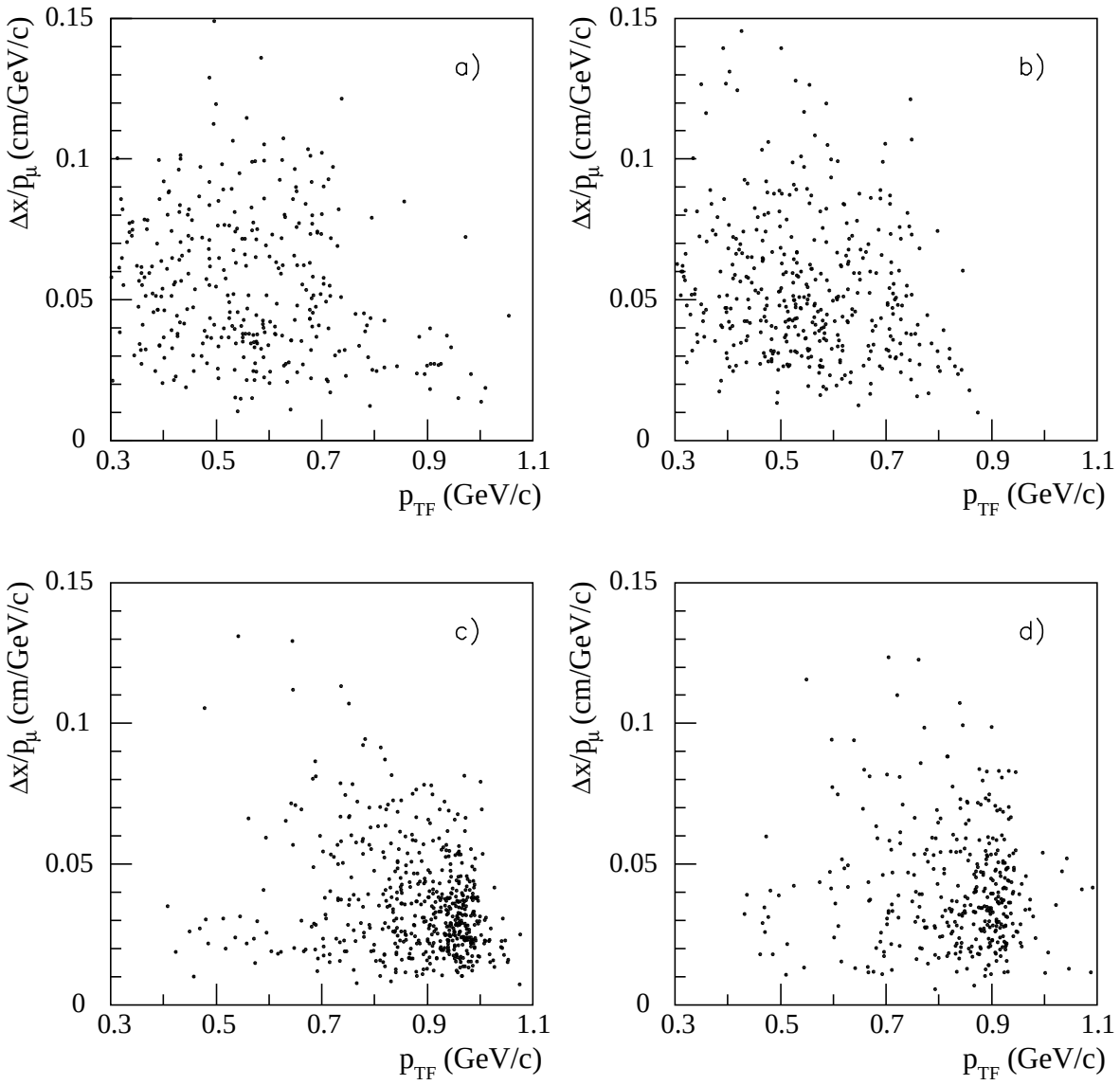

Figure 3: *Distributions of $\Delta x/p_\mu$ versus $p_{\rm TF}$ for the experimental data (a) and for simulated events featuring $c\bar{c}$ production (b), $D_s \to \mu\nu_\mu$ (c) and $D \to \mu\nu_\mu$ (d).*

Table 2: *Results of maximum-likelihood fits, with breakdown of statistical and systematic errors. The "other systematic" errors include the statistical errors on $\sigma(D)/\sigma(D_s)$, and the errors on M_D/M_{D_s}, τ_D/τ_{D_s} and $|V_{cd}|^2/|V_{cs}|^2$.*

	W92	Cu92	Cu93	Cu92+Cu93	all data
$N^{obs}_{D_s\to\mu\nu_\mu}$	2.7	5.3	9.1	14.9	18.0
$\sigma_{stat}(N^{obs}_{D_s\to\mu\nu_\mu})$	2.5	2.6	3.2	4.3	4.7
$\sigma_{syst}(N^{obs}_{D_s\to\mu\nu_\mu})$ from f_D/f_{D_s}	0.1	0.2	0.2	0.3	0.4
$\sigma_{syst}(N^{obs}_{D_s\to\mu\nu_\mu})$ from $B(D_s\to\varphi\pi)$	0.6	0.7	0.8	1.1	2.2
$\sigma_{syst}(N^{obs}_{D_s\to\mu\nu_\mu})$ (other syst.)	0.3	0.4	0.5	0.6	1.1

Table 3: *D_s muonic branching ratio relative to the decay $D_s \to \varphi_{(K^+K^-)}\pi$, with breakdowns of statistical and systematic errors. The systematic error on $N^{obs}_{D_s\to\mu\nu_\mu}$ induced by the error on $B(D_s \to \varphi_{(K^+K^-)}\pi)$ is not included in the total systematic error.*

	W92	Cu92	Cu93	Cu92+Cu93	all data
$\frac{B(D_s\to\mu\nu_\mu)}{B(D_s\to\varphi_{(K^+K^-)}\pi)}$	0.45	0.55	0.40	0.46	0.47
total statistical error	0.44	0.30	0.16	0.15	0.13
total systematic error	0.08	0.06	0.03	0.03	0.04
breakdown of errors:					
$D_s \to \mu\nu_\mu$ statistics	0.43	0.27	0.14	0.13	0.12
$D_s \to \mu\nu_\mu$ systematics from f_D/f_{D_s}	0.02	0.02	0.01	0.01	0.01
$D_s \to \mu\nu_\mu$ other systematics	0.05	0.04	0.02	0.02	0.03
$D_s \to \varphi_{(K^+K^-)}\pi$ statistics	0.11	0.14	0.06	0.06	0.05
$D_s \to \varphi_{(K^+K^-)}\pi$ systematics	0.06	0.05	0.02	0.02	0.03
$D_s \to \mu\nu_\mu$ systematics from $B(D_s \to \varphi\pi)$	0.10	0.07	0.04	0.03	0.06

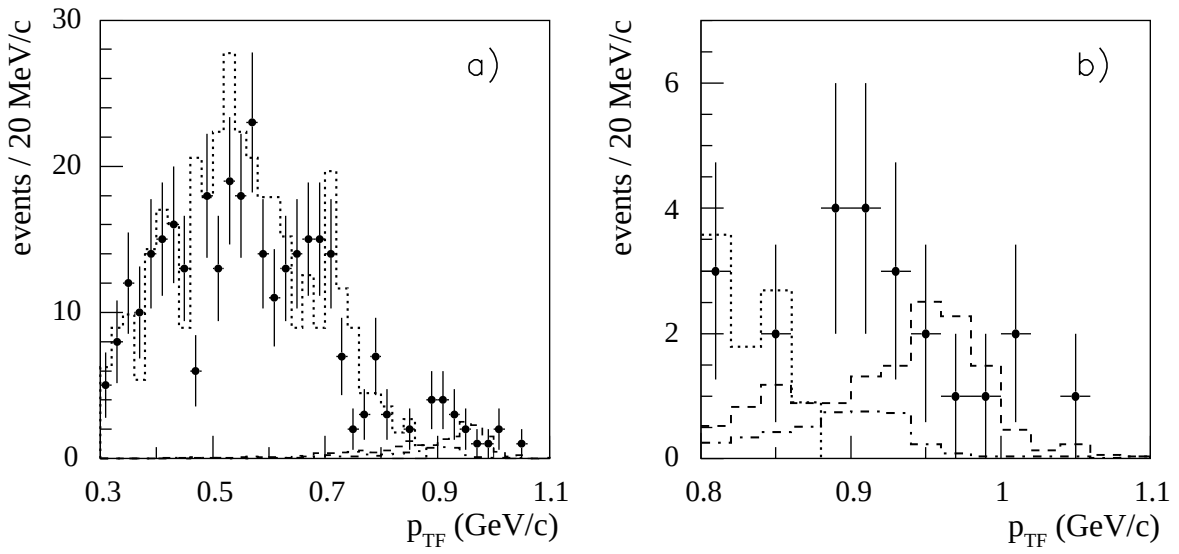

Figure 4: *a): p_{TF} distribution for all data sets together (data points with error bars). The dashed, dash-dotted and dotted histograms are the normalised contributions of $D_s \to \mu\nu_\mu$, $D \to \mu\nu_\mu$ and $c\overline{c}$ respectively. b): zoom of figure a) in the region containing most $D_s \to \mu\nu_\mu$ events.*

The number of $D_s \to \mu\nu_\mu$ decays was normalised to a sample of $D_s \to \varphi_{(K^+K^-)}\pi$ decays also measured in the present experiment [9]. The ratio $B(D_s \to \mu\nu_\mu)/B(D_s \to \varphi_{(K^+K^-)}\pi)$ was then calculated as:

$$\frac{B(D_s \to \mu\nu_\mu)}{B(D_s \to \varphi_{(K^+K^-)}\pi)} = \frac{N^{obs}_{D_s\to\mu\nu_\mu}}{\varepsilon_{D_s\to\mu\nu_\mu}} \times \frac{1}{N^{prod}_{D_s\to\varphi_{(K^+K^-)}\pi}}, \tag{4}$$

where $N^{prod}_{D_s\to\varphi_{(K^+K^-)}\pi}$ is the number of D_s mesons decaying according to $D_s \to \varphi\pi \to K^+K^-\pi$, this being $6770 \pm 1610 \pm 870$ for the W92 data set, $3710 \pm 910 \pm 320$ for Cu92 and $8470 \pm 1280 \pm 470$ for Cu93 [9]. This ratio is free from uncertainties due to the luminosity measurement and depends only weakly on the poor knowledge of the $D_s \to \varphi_{(K^+K^-)}\pi$ branching fraction. Table 3 shows the ratio of branching fractions for the W92, Cu92 and Cu93 samples separately and the result of the combined fits.

Using the world average for the branching fraction $B(D_s \to \varphi_{(K^+K^-)}\pi) = (1.77 \pm 0.44)\%$ [10], and taking into account the correlations of the errors on $B(D_s \to \varphi_{(K^+K^-)}\pi)$, the branching fraction $B(D_s \to \mu\nu_\mu)$ is found to be $(0.83 \pm 0.23 \pm 0.06 \pm 0.18)\%$, where the first error is statistical, the second is systematic and the third is the contribution of the error on $B(D_s \to \varphi_{(K^+K^-)}\pi)$ to the total systematic error.

This branching fraction, together with the current values of $|V_{cs}| = 0.9745 \pm 0.0008$ and $\tau_{D_s} = 0.467 \pm 0.017$ [10], can be used in equation (1), giving the D_s decay constant to be $f_{D_s} = 323 \pm 44 \pm 12 \pm 34$ MeV. This value is in the same range as, and has similar errors to, several existing measurements (see [10] for a complete list), but it is obtained using completely different techniques, both at the experimental level and in the analysis.

The WA92 experiment has used a narrow-pitched silicon microstrip detector to reconstruct fully $18.0 \pm 4.7 \pm 1.2$ $D_s \to \mu\nu_\mu$ decays in 350 GeV/c π^- interactions on copper and tungsten nuclei. The branching fraction of $D_s \to \mu\nu_\mu$ relative to the branching fraction $D_s \to \varphi\pi \to K^+K^-\pi$ was measured as:

$$\frac{B(D_s \to \mu\nu_\mu)}{B(D_s \to \varphi_{(K^+K^-)}\pi)} = 0.47 \pm 0.13 \pm 0.04 \pm 0.06.$$

From this result, the absolute muonic branching fraction and the decay constant of the D_s meson have been calculated as:

$$B(D_s \to \mu\nu_\mu) = (0.83 \pm 0.23 \pm 0.06 \pm 0.18)\%,$$

$$f_{D_s} = 323 \pm 44 \pm 12 \pm 34 \text{ MeV},$$

where the first error is statistical, the second is systematic and the third is the contribution of the error on the branching fraction $B(D_s \to \varphi_{(K^+K^-)}\pi)$ to the total systematic error.

The authors wish to thank Prof. Miron Livny and the Condor Team of the Computer Science Department, University of Wisconsin, Madison, for their help and collaboration on data processing; without the Condor system the present analysis would not have been possible.

References

[1] J.D. Richman and P.R. Burchat, Rev. Mod. Phys. 67 (1995) 893.

[2] M. Adamovich *et al.* (BEATRICE collaboration), Nucl. Instr. and Meth. A379 (1996) 252.

[3] A. Fassò *et al.*, Proc. IV International Conference on Calorimetry and their Applications, La Biodola, Italy (World Scientific, 1994) 493.

[4] H.-U. Bengtsson and T. Sjöstrand, Comput. Phys. Commun. 46 (1987) 43.

[5] M. Bengtsson and T. Sjöstrand, Comput. Phys. Commun. 43 (1987) 367.

[6] GEANT Detector Description and Simulation Tool, CERN Program Library Long Writeup W5013 (1994).

[7] J.C. Lassalle *et al.*, Nucl. Instr. and Meth. 176 (1980) 371.

[8] MINUIT Function Minimization and Error Analysis, CERN Program Library Long Writeup D506 (1994).

[9] M. Adamovich *et al.* (BEATRICE collaboration), Nucl. Phys. B495 (1997) 3.

[10] C. Caso *et al.* (Particle Data Group), Eur. Phys. Jour. C3 (1998) 1.

[11] J. Flynn and C. Sachrajda, Heavy Flavours II, edited by A. Buras and M. Linder, World Scientific, Singapore (1998) 402.